

Sub-diffraction-limit semiconductor resonators operating on the fundamental magnetic resonance

E. Strupiechonski, G. Xu, M. Brekenfeld, Y. Todorov, N. Isaac et al.

Citation: *Appl. Phys. Lett.* **100**, 131113 (2012); doi: 10.1063/1.3697660

View online: <http://dx.doi.org/10.1063/1.3697660>

View Table of Contents: <http://apl.aip.org/resource/1/APPLAB/v100/i13>

Published by the [American Institute of Physics](http://www.aip.org).

Related Articles

Planar superconducting resonators with internal quality factors above one million

Appl. Phys. Lett. **100**, 113510 (2012)

Design and testing of multi-standard waveguide couplers

Rev. Sci. Instrum. **83**, 034702 (2012)

Analysis of mid-range electric power transfer based on an equivalent circuit model

J. Appl. Phys. **111**, 07E733 (2012)

An analysis method for asymmetric resonator transmission applied to superconducting devices

J. Appl. Phys. **111**, 054510 (2012)

Improved fake mode free plane-wave expansion and three planar-slab waveguides method

J. Appl. Phys. **111**, 053103 (2012)

Additional information on *Appl. Phys. Lett.*

Journal Homepage: <http://apl.aip.org/>

Journal Information: http://apl.aip.org/about/about_the_journal

Top downloads: http://apl.aip.org/features/most_downloaded

Information for Authors: <http://apl.aip.org/authors>

ADVERTISEMENT

NEW!

iPeerReview

AIP's Newest App



Authors...
Reviewers...

Check the status of
submitted papers remotely!

AIP | Publishing

Sub-diffraction-limit semiconductor resonators operating on the fundamental magnetic resonance

E. Strupiechonski,¹ G. Xu,¹ M. Brekenfeld,¹ Y. Todorov,² N. Isac,¹ A. M. Andrews,³ P. Klang,³ C. Sirtori,² G. Strasser,³ A. Degiron,¹ and R. Colombelli^{1,a)}

¹Institut d'Electronique Fondamentale, Univ. Paris Sud, UMR8622 CNRS, 91405 Orsay, France

²Laboratoire MPQ, Université Paris Diderot, CNRS-UMR 7162, 75013 Paris, France

³Institute for Solid-State Electronics, Vienna University of Technology, 1040 Wien, Austria

(Received 27 December 2011; accepted 1 March 2012; published online 27 March 2012)

We demonstrate semiconductor terahertz (THz) resonators with sub-wavelength dimensions in *all three dimensions* of space. The maximum confinement is obtained for resonators with a diameter of 13 μm , which operate at a wavelength of $\approx 272 \mu\text{m}$. This corresponds to a $\lambda_{\text{eff}}/6$ confinement, where λ_{eff} is the wavelength inside the material (or $\lambda/20$, if the free space wavelength is considered). These highly sub-wavelength devices operate on the fundamental magnetic resonance, which corresponds to the fundamental oscillation mode of split-ring resonators and is usually inactive in purely optical resonators. In this respect, these resonators are another step towards the hybridization of optics and electronics at THz frequencies. As a proof of principle for cavity quantum electrodynamics experiments, we apply these resonators to THz intersubband polaritons.

© 2012 American Institute of Physics. [<http://dx.doi.org/10.1063/1.3697660>]

Optical oscillators—commonly known as optical resonators—are constrained to a minimum dimension set by the wavelength.¹ It is the so called diffraction limit and it constrains the resonator dimension to a minimum value of essentially $\lambda/2n_{\text{eff}}$ in *at least one dimension of space*, where n_{eff} is the effective index of the optical mode. This constraint only partially limits the total volume, since in the other two dimensions, the resonator can be sub-wavelength. For this reason, several demonstrations have been given recently of lasers with very small and sub-wavelength modal volumes. These demonstrations cover a large spectral range, with results spanning the visible,^{2,3} the near-infrared,^{4–7} and the THz frequency ranges.⁸ In particular in the THz range, the use of metal-semiconductor-metal structures⁹ is very convenient because very thin structures can be employed (TEM modes have no frequency cut-off in metal-metal waveguides).¹⁰

On one hand, freeing optical resonators from the diffraction limit is a conceptually gratifying achievement. On the other hand, it can lead to devices with even more extreme electromagnetic field confinements, a trend which is of importance for cavity quantum electrodynamics (c-QED).¹¹ As a matter of fact, this problem is partially addressed by metamaterials.¹² These artificial objects exhibit user-designed electromagnetic functionalities thanks to the averaged response of extremely sub-wavelength resonators usually termed meta-atoms. The archetypical meta-atom is the splitting resonator (SRR, see right part of Fig. 1(b)).¹³ It can easily exhibit sub-wavelength dimensions of $\approx \lambda/10$ or less *in all three dimensions of space* since the periodic energy exchange typical of any oscillator is mediated by a *real electric current* (arrow in Fig. 1(b)), and not—as in standard optical resonators—by the time-varying terms of Maxwell's equations (like the displacement current $\partial\mathbf{D}/\partial t$). SRRs and related geometries also comprise a capacitive region with

almost uniform electric field (E-field region with red arrows in Fig. 1(b)). Under resonant conditions, the amplitude of the electric field becomes extremely large within the capacitive gap, making the structure highly sensitive to any material placed in this region. This property is often exploited in the context of active functional meta-materials which are typically obtained by inserting a semiconductor or a nonlinear substance in the resonator gap^{13–19,29,30} in order to tune the collective response of the effective medium. Here, we show that SRRs with a semiconductor active core in the E-field region have an enormous potential as standalone optoelectronic devices with dimensions much smaller than $\lambda/2$ in the three dimensions of space.

In this paper, we study semiconductor resonators which are *topologically* equivalent to a SRR resonator and which can host an active semiconductor core. We compare the oscillating modes in a semiconductor loaded circular patch-cavity resonator (Figs. 1(a) and 1(c)), with the electromagnetic modes in a SRR-like structure with semiconductor core (Figs. 1(b) and 1(d)). We then embed quantum well structures in the SRR-like resonators and study cavity quantum-electrodynamic effects in the form of Rabi splitting in the coupled system.

Figure 1(c) shows the SEM figure of a standard circular patch-cavity resonator.²⁰ The lowest energy photonic eigenmode is the dipolar mode (Fig. 1(e)). When an electrical connection is provided between the opposing metallic plates of the patch-cavity resonator (SEM image in Fig. 1(d)), charge exchange between the opposing plates is allowed. This activates a resonance with monopolar electric field distribution, where the plates have electric charges with opposite signs. The simulation in Fig. 1(g) shows its electric field distribution. While the dipolar mode still exists in SRR-like resonators (Fig. 1(f)), the new lowest energy eigenmode is the monopolar one, which is instead forbidden by the charge conservation law in standard patch cavities. In fact, the

^{a)}Electronic mail: raffaele.colombelli@u-psud.fr.

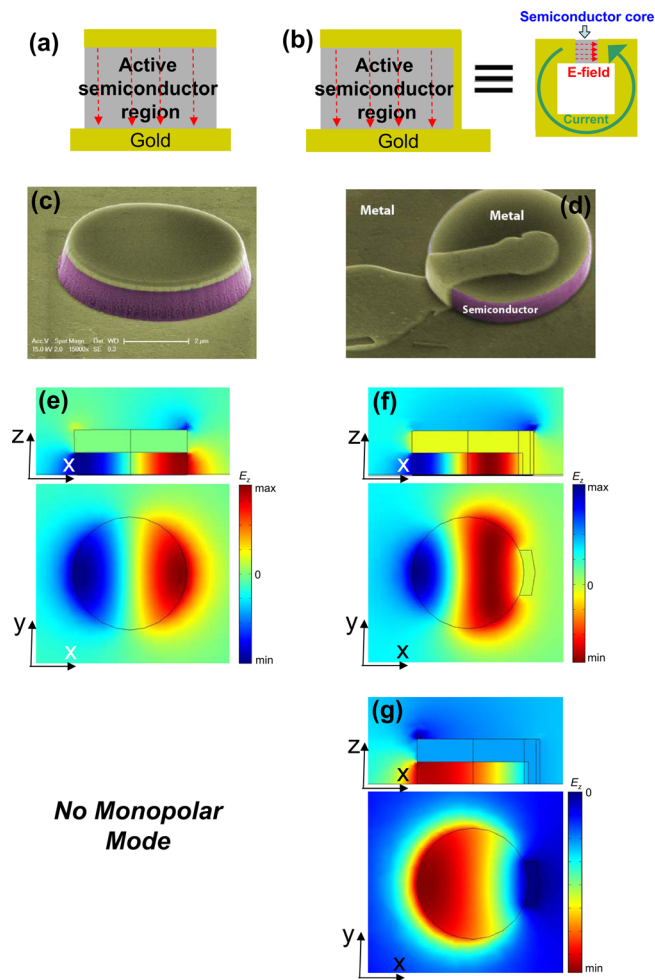


FIG. 1. (a) and (b) Scheme of a standard patch-cavity resonator (a) and a SRR-like resonator able to operate on the monopolar resonance (b). (c) SEM image of a typical round patch cavity. (d) SEM image of a typical SRR-like resonator. (e) and (f) Side/top view of the field distribution (electric field component orthogonal to the metallic contacts, E_z) for the *dipolar* mode of the standard (e) and SRR-like (f) resonators. (g) Side/top view of the field distribution (electric field component orthogonal to the metallic contacts, E_z) for the *monopolar* mode of the SRR-like resonator. Note: the monopolar mode is absent/inactive in a standard patch cavity.

monopolar field has an electrostatic nature:¹³ the electric field oscillates because it is mainly driven by alternating currents in the electrical connection between the opposing metallic plates. In the language of meta-materials, this means operating the device on the fundamental magnetic dipolar resonance of the SRR: this is the resonator mode which yields the highest sub-wavelength confinement within the capacitive gap. Note that the monopolar mode has a net magnetic moment along the y -direction so it can couple—even at normal incidence—with electromagnetic waves with a non-zero magnetic field component along the y axis.

We have fabricated arrays of standard (Fig. 1(c)) and SRR-like (Fig. 1(d)) devices with different diameters, encompassing a $1\text{-}\mu\text{m}$ -thick SI-GaAs slab between metallic (Ti/Au) mirrors. A SEM image of a typical array is reported in the inset of Fig. 2(a). Standard wafer-bonding techniques, followed by contact optical lithography and ICP etching, have been employed. Reflectivity measurements in the THz spectral region allow us to test the optical response of the structures and identify the frequency of

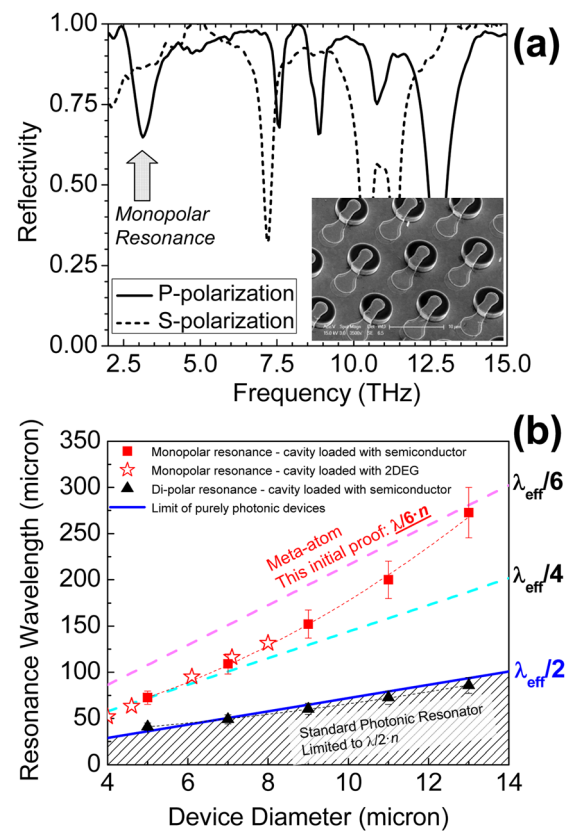


FIG. 2. (a) Typical reflectivity measurement. A polarized beam from a Glan-lamp of a Bruker interferometer (IFS66) is focused on the sample and the reflected beam is measured with a liquid-He cooled bolometer. The measured device is a SRR-like cavity with $6\text{-}\mu\text{m}$ diameter (an SEM image of the sample is reported in the inset). The solid line corresponds to the polarization which couples with the monopolar resonance, marked by a grey arrow. The dashed line corresponds to the 90° -rotated polarization: the monopolar mode is not active, and the degeneracy breaking of the dipolar modes (at a frequency of ≈ 7.5 THz) is clearly observed. (b) Plot of the fundamental resonator wavelength as a function of the device diameter, for standard (black triangles) and SRR-like resonators (red squares and open stars). The straight lines materialize the $\lambda/2$, $\lambda/4$, and $\lambda/6$ confinement regions. The full blue line marks the limit of purely photonic devices. The data prove that standard resonators are confined to the limit of purely photonic devices, while the SRR-like resonators can reach $\lambda/6$ confinement in all three dimensions of space. The data are obtained with room-temperature reflectivity measurements.

the resonant modes *via* sharp resonances in the reflectance spectra.²¹ Fig. 2(a) shows a typical measurement performed at 45° incidence of a $6\text{-}\mu\text{m}$ -diameter SRR-like cavity. In this experiment, the plane of incidence passes through the x and z axes. When the polarization of the incident beam is such that the B-field is parallel to the plates and couples with the inductive section of the SRR, the monopolar, fundamental resonance is clearly observed at a frequency of ~ 3.2 THz. The monopolar mode is also well separated in frequency from the dipolar modes, which appear only at ≈ 7.5 THz.

Figure 2(b) shows the results of a systematic study at room-temperature of the fundamental resonance of standard and SRR-like resonators: it plots the resonance *wavelength* as a function of the device diameter, which is the largest device dimension since the semiconductor slab thickness is $\approx 1\text{ }\mu\text{m}$. The lowest frequency resonance of standard cavities is dipolar (black triangles): the data lie on the $\lambda = 2 \cdot n \cdot d$ line

(n is the refraction index of GaAs, which is experimentally determined as ≈ 3.6 from the linear fit to the data in Fig. 2(b); d is the device diameter). The dashed area below this line materializes the region accessible with standard optical resonators, which are rigorously constrained by the fundamental diffraction limit.

On the other hand, the lowest frequency resonance of SRR-like resonators is monopolar (solid red squares, and open red stars): the data clearly break the diffraction limit and lie in the region comprised between $\lambda/4$ and $\lambda/6$ confinements (dashed and dashed-dotted lines). The maximum confinement of $\lambda/6$ is obtained for resonators with diameter $13\ \mu\text{m}$. Note the difference: for this same dimension, standard cavities feature a resonant wavelength of $86\ \mu\text{m}$, while SRR-like cavities operate at $273\ \mu\text{m}$. This corresponds to a record-low active effective volume of only $V_{\text{eff}} = 0.0025 \cdot (\lambda/2n)^3$.

Fig. 2(b) suggests that the confinement is decreased for smaller cavities. This effect is not fundamental: it is instead due to finite-size effects originating from processing limitations. The devices are fabricated with optical lithography, hence the minimum achievable width of the electrical connection between the opposing metallic plates is $\sim 1.5\ \mu\text{m}$ (Fig. 2(a), inset). When the cavity size is of the same order, the side contact behaves more as a vertical mirror metallic condition. The system tends to the theoretical value of $\lambda/4$, which can be obtained by applying the method of the image charges,²² but when the resonator size becomes larger, the side contact behaves like a one-dimensional wire. The resonance frequency—as in an SRR resonator—is essentially set by the wire inductance and extremely sub-wavelength dimensions can be attained. In this work, we are possibly limited to $\lambda/6$ by the *wire* width.

As a proof of principle that these cavities are promising for c-QED applications, we prepared a 2nd set of devices where the slab of SI-GaAs is replaced by a 2D electron gas, made of a $1.3\text{-}\mu\text{m}$ -thick slab of GaAs/AlGaAs quantum wells. The semiconductor structure used is the same as in Ref. 23 and has been designed so that an intersubband (ISB) transition of energy $\hbar\omega_{21} \approx 12.4\ \text{meV}$ (3 THz) can be activated at low temperature. At high temperature, the ISB transition is not active because electrons populate several energy levels and exhibit similar density on the two subbands under consideration. The 2DEG behaves as a slab of lightly doped GaAs. This allows one to determine the cavity resonances with room-temperature reflectivity measurements (empty stars symbols in Fig. 2(b)). The figure suggests that the SRR-like cavity with a diameter of only $6\ \mu\text{m}$ has a resonance that coincides with the 3 THz ISB transition. Hence, it is the best candidate to measure the Rabi splitting of the *intersubband polaritons* resulting from the strong-coupling between the SRR resonance and the ISB transition when the temperature is lowered. These intersubband polaritons are the new eigenmodes of the system and arise when the coupling between the SRR mode and matter increases beyond the damping rates of both cavity and material excitation. Furthermore, the coupling frequency—usually called Rabi frequency Ω_{Rabi} —becomes the characteristic time of the system.¹¹

The relevant measurements are reported in Fig. 3, which shows reflectivity measurements—at 45° incidence—on the

SRR-like resonator with $6\text{-}\mu\text{m}$ diameter for heat-sink temperatures decreasing from 150 K to 4 K. Below 80 K, the resonant feature at ~ 3.2 THz in the reflectivity spectra splits in two modes, with similar full width at half maximum (FWHM), which correspond to the lower and upper ISB polariton states. The experimentally measured Rabi splitting—defined as $2\Omega_{\text{Rabi}} = \omega_{\text{upper}} - \omega_{\text{lower}}$ —is 1.51 THz (Fig. 3, spectrum taken at 5 K).

Our cavity is not a pure optical resonator but a hybrid device operating in AC mode. From a conceptual point of view, the observed polaritons have a different nature than those formed in standard c-QED experiments, because it is not photons that directly couple with the ISB transition but a resonance involving real electrical currents. In this regard, our results can be seen as a case of hybrid interaction between meta-atoms and matter, similar to the hybridization between SRRs and the gyromagnetic resonance of a ferrite material reported in Ref. 24 at microwave frequencies or between nanoscale metamaterials and phonons.²⁸

An extremely important figure of merit in polaritonics is the ratio $2 \cdot \Omega_{\text{Rabi}}/\omega_{21}$, which materializes the strength of the anti-resonant terms in the polariton Hamiltonian.²⁵ When Ω_{Rabi} becomes a sizeable fraction of the bare material excitation, we enter the *ultra-strong* coupling regime, where fundamental phenomena (dynamical Casimir effect²⁶ and correlated photons generation) can in principle become accessible.²⁷ The maximum $2 \cdot \Omega_{\text{Rabi}}/\omega_{21}$ ratio reported to date (without application of a magnetic field) is 47% and it was demonstrated in Ref. 23. In this work, we have employed the same structure, and—using the monopolar resonators—we increased this value by 7%. This (light) improvement possibly stems from the increased electromagnetic confinement factor of the monopolar resonance and also from the increased index contrast due to the semiconductor etching, which is instead absent in Ref. 23.

In conclusion, we have demonstrated semiconductor THz resonators with a sub-wavelength confinement of at

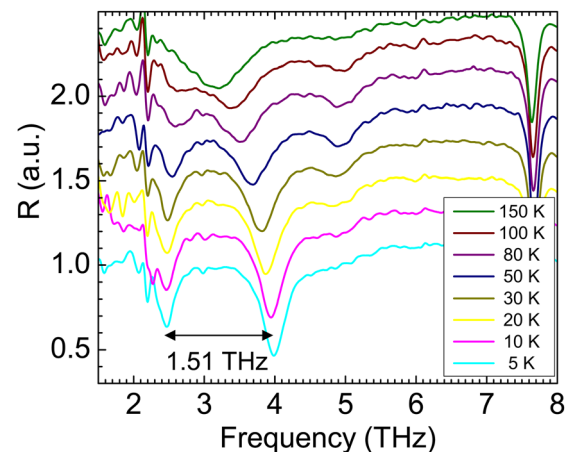


FIG. 3. Reflectivity measurements at different heat-sink temperatures of a SRR-like resonator with $6\text{-}\mu\text{m}$ -diameter, with the slab of SI-GaAs replaced by a 2D electron gas, made of a $1.3\text{-}\mu\text{m}$ -thick slab of GaAs/AlGaAs quantum wells. The ISB transition—which activates at low temperatures—is centered at a frequency of ≈ 3 THz, in resonance with the monopolar mode of the resonator. Lowering the temperature yields a mode splitting, which clearly demonstrates the strong-coupling regime. The measured Rabi splitting is ≈ 1.51 THz.

least $\lambda/6$ in all three dimensions of space, and a record-low effective volume of $V_{\text{eff}} = 0.0025 \cdot (\lambda/2 \cdot n)^3$ has been achieved. These extremely sub-wavelength devices operate on the fundamental oscillation mode of split-ring resonators and it is not accessible in purely optical resonators. An initial application to c-QED phenomena has been given by demonstrating the ultra-strong coupling regime between the fundamental monopolar mode and matter in a semiconductor system, with a slightly increased coupling strength with respect to a dipolar mode. This concept could be easily transposed to a laser device by inserting the gain medium in the region where the electric field is confined, resulting in lasers with highly sub-wavelength dimensions in all three dimensions of space.

We thank I. Sagnes and U. Gennser for providing the GaAs epitaxial layer, and S. Dhillon and P. Cavalié for help and discussions. The device fabrication has been performed at the nano-center CTU-IEF-Minerve, partially funded by the “Conseil Général de l’Essonne.” This work was partially supported by the French National Research Agency (Project PNANO “Thinke-Pinke”) and by the RTRA project “Phlare.” The authors acknowledge partial support from the Austrian FWF project IRON (F2503-N17) and from the PLATON project 35N within the Austrian NANO initiative. M. Brekenfeld acknowledges support from the Ecole Polytechnique (member of ParisTech). MPQ laboratories acknowledge partial support from Region Île-de-France.

¹M. Born and E. Wolf, *Principles of Optics: Electromagnetic Theory of Propagation, Interference and Diffraction of Light* (Cambridge University Press, 1997).

²M. Noginov *et al.*, *Nature* **460**, 1110–1112 (2009).

³R. F. Oulton, V. J. Sorger, T. Zentgraf, R.-M. Ma, C. Gladden, L. Dai, G. Bartal, and X. Zhang, *Nature* **461**, 629 (2009).

⁴H. Park *et al.*, *Science* **305**, 1444–1447 (2004).

- ⁵J. Scheuer, W. Green, G. DeRose, and A. Yariv, *Appl. Phys. Lett.* **86**, 251101 (2005).
- ⁶K. Nozaki and T. Baba, *Appl. Phys. Lett.* **88**, 211101 (2006).
- ⁷M. Hill *et al.*, *Nat. Photonics* **1**, 589–594 (2007).
- ⁸C. Walther, G. Scalari, M. Amanti, M. Beck, and J. Faist, *Science* **327**, 1495 (2010).
- ⁹K. Unterrainer, R. Colombelli, C. Gmachl, F. Capasso, H. Y. Hwang, A. M. Sergent, D. L. Sivco, and A. Y. Cho, *Appl. Phys. Lett.* **80**, 3060 (2002).
- ¹⁰A. Yariv, *Quantum Electronics*, 3rd ed. (Wiley, 1989).
- ¹¹*Proceedings of the International School of Physics Enrico Fermi, Course CL*, edited by B. Deveaud, A. Quattropani, and P. Schwendimann (IOS, Amsterdam, 2003).
- ¹²D. R. Smith *et al.*, *Phys. Rev. Lett.* **84**, 4184 (2000).
- ¹³J. B. Pendry, A. J. Holden, D. J. Robbins, and W. J. Stewart, *IEEE Trans. Microwave Theory Tech.* **47**, 2075 (1999).
- ¹⁴I. V. Shadrivov, S. K. Morrison, and Y. S. Kivshar, *Opt. Express* **14**, 9344 (2006).
- ¹⁵H.-T. Chen, W. J. Padilla, J. M. O. Zide, A. C. Gossard, A. J. Taylor, and R. D. Averitt, *Nature* **444**, 597 (2006).
- ¹⁶A. Degiron, J. J. Mock, and D. R. Smith, *Opt. Express* **15**, 1115 (2007).
- ¹⁷D. Huang, A. Rose, E. Pourtrina, S. Larouche, and D. R. Smith, *Appl. Phys. Lett.* **98**, 204102 (2011).
- ¹⁸A. R. Katko, S. Gu, J. P. Barrett, B.-I. Popa, G. Shvets, and S. A. Cummer, *Phys. Rev. Lett.* **105**, 123905 (2010).
- ¹⁹A. A. Tavallae, P. Hon, K. Mehta, T. Itoh, and B. S. Williams, *IEEE J. Quantum Electron.* **46**, 1091 (2010).
- ²⁰C. Manolatou and F. Rana, *IEEE J. Quantum Electron.* **44**, 435 (2008).
- ²¹Y. Todorov, L. Tosetto, J. Teissier, A. M. Andrews, P. Klang, R. Colombelli, I. Sagnes, G. Strasser, and C. Sirtori, *Opt. Express* **18**, 13886 (2010).
- ²²J. D. Jackson, *Classical Electrodynamics*, 3rd ed. (Wiley, 1998).
- ²³Y. Todorov, A. M. Andrews, R. Colombelli, S. De Liberato, C. Ciuti, P. Klang, G. Strasser, and C. Sirtori, *Phys. Rev. Lett.* **105**, 196402 (2010).
- ²⁴J. N. Gollub, J. Y. Chin, T. J. Cui, and D. R. Smith, *Opt. Express* **17**, 2122 (2009).
- ²⁵C. Ciuti, G. Bastard, and I. Carusotto, *Phys. Rev. B* **72**, 115303 (2005).
- ²⁶C. M. Wilson, G. Johansson, A. Pourkabirian, M. Simoen, J. R. Johansson, T. Duty, F. Nori, and P. Delsing, *Nature* **479**, 376 (2011).
- ²⁷C. Ciuti and I. Carusotto, *Phys. Rev. A* **74**, 033811 (2006).
- ²⁸D. J. Shelton, I. Brener, J. C. Ginn, M. B. Sinclair, D. W. Peters, K. R. Coffey, and G. D. Boreman, *Nano Lett.* **11**, 2104 (2011).
- ²⁹X. Wu, S. K. Gray, and M. Pelton, *Opt. Express* **18**, 23633–23645 (2010).
- ³⁰P. Weis, J. L. Garcia-Pomar, R. Beigang, and M. Rahm, *Opt. Express* **19**, 23573 (2011).